  DOI 10.1515/HTMP.2011.122

New Poly(amide-imide)/Nanocomposites Reinforced Silicate Nanoparticles Based on *N*-pyromellitimido-*L*-phenyl Alanine Containing Ether Moieties

Khalil Faghihi,[1,*] **Meisam Shabanian**[2] **and Ehsan Dadfar**[1]

[1] Polymer Research Laboratory, Department of Chemistry, Faculty of Science, Arak Branch, Islamic Azad University, Arak, Iran

[2] Young Researchers Club, Arak Branch, Islamic Azad University, Arak, Iran

Abstract. A series of Poly(amide-imide)/montmorillonite nanocomposites containing *N*-pyromellitimido-*L*-phenyl alanine moiety in the main chain were synthesized by a convenient solution intercalation technique. Poly(amide-imide) (PAI) **5** as a source of polymer matrix was synthesized by the direct polycondensation reaction of *N*-pyromellitimido-*L*-phenyl alanine **3** with 4,4'-diamino diphenyl ether **4** in the presence of triphenyl phosphite (TPP), $CaCl_2$, pyridine and *N*-methyl-2-pyrrolidone (NMP). The resulting nanocomposite films were characterized by Fourier transform infrared spectra (FT-IR), X-ray diffraction (XRD), scanning electron microscopy (SEM) and thermogravimetric analysis (TGA). The results showed that organo-modified clay was dispersed homogeneously in PAI matrix. TGA indicated an enhancement of thermal stability of new nanocomposites compared with the pure polymer.

Keywords. Poly(amide-imide), nanocomposite, thermal properties, ether moieties.

PACS®(2010). 81.05.Qk.

1 Introduction

During the past decade, polymer-clay nanocomposites (PCNs) consisting of inorganic nanolayers clay and organic polymers have attracted a great interest, because of their excellent properties compared to neat polymer [1–3] Different studies in this field have discovered that dispersion of small portions of inorganic clay, improve physical and chemical properties of organic polymers, such as thermal stability [4], mechanical strength [5], solvent resistance [6], flame retardation [7], ionic conductivity [8], corrosion resistance [9, 10], gas barrier properties [11, 12], and dielectric properties significantly [13–15] Among many engineering polymers, aromatic polyimides (PIs) are well known as hightemperature polymers that exhibit excellent mechanical strength and thermal stability. Several approaches such as introduction of flexible bridging linkages into the polymer backbone such as –NHCO–, –O–, and –SO_2– [16–18], are incorporated into the polymer backbone due to the altering crystallinity and intermolecular interactions [19, 20]. Among them, polyamide-imide (PAI) is the most successful material, which combines the advantages of high-temperature stability and processability [21–24]. Performance of polymer-clay nanocomposites (PCNs) depends on dispersion and spacing between clay layers. Two types of polymer-clay nanocomposites (PCNs) can be obtained, depending on the preparation method and the nature of the components used, including polymer matrix, layered silicate and organic cation: intercalated and exfoliated [25,26]. The improvement of physical and chemical properties occurs even with the addition of low percentages of organically modified clay; the properties are enhanced when the clay platelets are exfoliated and unsystematically dispersed in a polymer matrix. In this article two PAI-nanocomposite films with 5 and 10% silicate particles containing chiral-pyromellitimido-*L*-phenyl alanine moiety in the main chain was prepared by using a convenient solution intercalation technique.

2 Experimentals

2.1 Materials

4,4'-diamino diphenyl ether, triphenyl phosphite (TPP), pyromellitimido anhydrate, L-phenyl alanine and $CaCl_2$, were purchased from Merck Chemical Company, pyridine and *N*-methyl-2-pyrrolidone (NMP) were purchased from Fluka Chemical Co. (Switzerland), then used without further purification Purified montmorillonite Cloisite® Na^+ and the organically-modified Cloisite® 20A supplied by

* **Corresponding author:** Khalil Faghihi, Department of Chemistry, Faculty of Science, Arak Branch, Islamic Azad University, Arak, 567-38135, Iran; E-mail: k-faghihi@araku.ac.ir.

Received: May 12, 2011. Accepted: June 1, 2011.

Type of clay	Organic modifier	Concentration of organic modifier [meq/100 g clay]	Interlayer distance (nm)
Cloisite® 20A	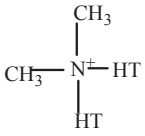	95	1.77

Table 1. Organic modifiers and interlayer distance of the clays.

Southern Clay Products (TX), were used as polymer nanoreinforcement. The organic modifiers and the interlayer distance of the clays are shown in Table 1 to account the structural modifications of the functional points

2.2 Measurements

^{1}H-NMR spectrum was recorded on a Bruker 300 MHz instrument (Germany). Fourier transform infrared (FTIR) spectra were recorded on Galaxy Series FTIR 5000 spectrophotometer (England). UV-visible spectra were recorded at 298 K in the 250–800 nm spectral regions with a Perkin Elmer Lambda 15 spectrophotometer in NMP solution using cell lengths of 1 cm. Thermal Gravimetric Analysis (TGA and DTG) data were taken on a Mettler TA4000 System under N_2 atmosphere at a rate of 10 K/min. The morphology of nanocomposite film was investigated on Canbridge S260 scanning electron microscope (SEM).

2.3 Monomer Synthesis

N-pyromellitimido-*L*-phenyl alanine **3** was prepared according to a typical procedure was shown in figure 1[27].

2.4 Polymer Synthesis

Into a 100 mL round bottomed flask were placed a mixture of *N*-pyromellitimido-*L*-phenyl alanine **3** (0.0006 mol), 4,4'-diamino diphenyl ether **4** (0.0006 mol), 0.30 g of calcium chloride, 2.4 mL of triphenyl phosphite, 0.7 mL of pyridine and 7.0 mL NMP. The mixture was heated for 1 h at 353 K, 2 h at 373 K and then refluxed at 393 K for 8 h until a viscous solution was formed. Then it was cooled to room temperature and 80 mL of methanol was added to reaction mixture. The precipitate was formed, filtered off and washed with methanol. The resulting polymers 5 were dried under vacuum. The inherent viscosity of this soluble PA **5** was 0.32 dL/g.

2.5 PAI-Nanocomposite Synthesis 5a and 5b

PAI-nanocomposites **5a** and **5b** were produced by solution intercalation method, in two different amounts of organoclay particles (5 and 10-mass%) were mixed with appropriate amounts of PAI solution in *N*-methyl-2-pyrrolidone (NMP) to yield particular nanocomposite concentrations. To control the dispersibility of organoclay in poly(amide-imide) matrix, constant stirring was applied at 298 K for 24 h. Nanocomposite films were cast by pouring the solutions for each concentration into petri dishes placed on a leveled surface followed by the evaporation of solvent at 343 K for 12 h. Films were dried at 253 K under vacuum to a constant weight. Figure 1 shows the flow sheet diagram and synthetic scheme for PAI-nanocomposites film **5a** and **5b**.

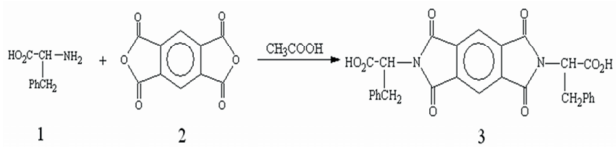

Figure 1. Synthetic route of *N*-pyromellitimido-*L*-phenyl alanine **3**.

2.6 The Water Absorption Analysis

The water absorption of PAI-nanocomposite films was carried out using a procedure under ASTM D570-81 [28]. The films were dried in a vacuum oven at 353 K to a constant weight and then weighed to get the initial weight (W_0). The dried films were immersed in deionized water at 298 K. After 24 h, the films were removed from water and then they were quickly placed between sheets of filter paper to remove the excess water and films were weighed immediately. The films were again soaked in water. After another 24 h soaking period, the films were taken out, dried and weighed for any weight gain. This process was repeated again and again till the films almost attained the constant weight. The total soaking time was 168 h and the samples were weighed at regular 24 h time intervals to get the final weight (W_f). The percent increase in weight of the samples was calculated by using the formula $(W_f - W_0)/W_0$.

3 Results and Discussion

3.1 Monomer Synthesis

N-pyromellitimido-*L*-phenyl alanine **3** was synthesized by the condensation reaction of one equimolar of Pyromellitic

anhydride **1** with one equimolar of L-phenyl alanine **2** in an acetic acid solution (Figure 1).

3.2 Polymer Synthesis

poly(amide-imide)s **5** was synthesized by the direct solution polycondensation reaction of an equimolar mixture of diacid 3, an equimolar mixture of diamine **4** by using triphenyl phosphate (TPP) and pyridine as condensing agents (Figure 2). PAI **5** was obtained in good yield (95%) and inherent viscositiy (0.32 dLg^{-1}). The structure of resulting polymer **5** was confirmed as PAI by using FTIR spectroscopy and elemental analyses. The resulting polymer have absorption band between 1771 and 1602 cm^{-1} due to imide and amide carbonyl groups. Absorption bands around 1379 cm^{-1} and 722 cm^{-1} demonstrated the presence of the imide heterocyclic absorption in these polymers. Also absorption band of amide group appeared at 3385 cm^{-1} (N-H stretching). The elemental analysis value of the resulting polymer was in good agreement with the calculated values for the proposed structure.

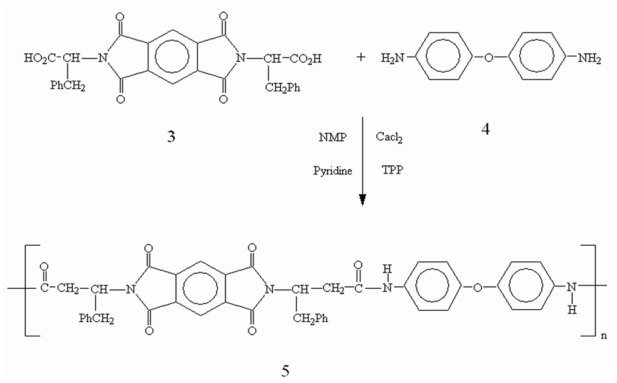

Figure 2. Synthetic route of PAI **5**.

3.3 PAI-nanocomposite Films

PAI-nanocomposite films were transparent and yellowish brown in color. The incorporation of organoclay changed the color of films to dark yellowish brown. Moreover, a decrease in the transparency was observed at higher clay contents. Figure 3 shows the flowsheet diagram and synthetic scheme for PAI-nanocomposites film **5a** and **5b**.

3.4 Characterization

3.4.1 FT-IR Spectroscopy Analyses

FT-IR spectroscopy spectra of PAI-nanocomposite films **5a** and **5b** showed the characteristic absorption bands of the Si-O and Mg-O moieties at 1009 and 465 cm^{-1} respectively. The incorporation of organic groups in PAI-nanocomposite films was confirmed by the presence of peaks at 1771, 1721, 1377, 720 (imide rings) and 1680 (amide carbonyl group) (Figure 4).

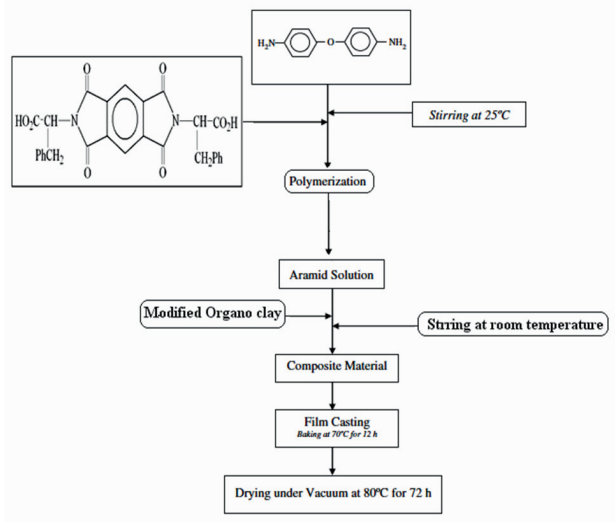

Figure 3. Flow sheet diagram for the synthesis of PAI-nanocomposites film **5a** and **5b**.

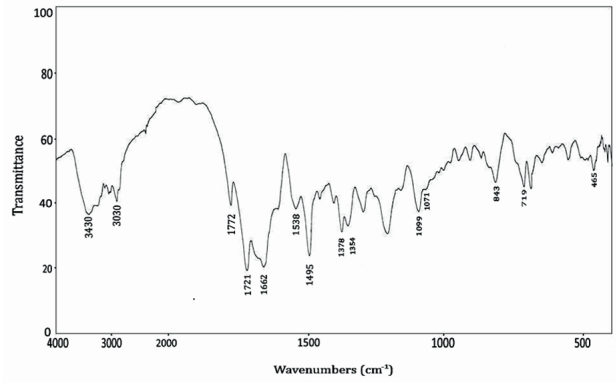

Figure 4. FTIR spectrum of PAI-nanocomposite films **5a**.

3.4.2 X-ray Diffraction Analysis

Figure 5 shows the XRD patterns of PAI-nanocomposite films **5a** and **5b** containing 5 and 10-mass% of silicate particles. The result reveals an increased d-spacing from 1.00 nm (8.93°) of Na-MMT to 1.49 nm (5.30°) of PAI-nanocomposite film (5 mass%) and (4.85°) of PAI-nanocomposite film (10 mass%). These results indicated significant expansion of the silicate layer after insertion PAI chains. The shift in the diffraction peaks PAI-nanocomposite films confirms that intercalation has been taken place. This is direct evidence that PAI-nanocomposites have been formed as the nature of intercalating agent also affects the organoclay dispersion in the polymer matrix. Usually there are two types of nanocomposites depending upon the dispersion of clay particles.

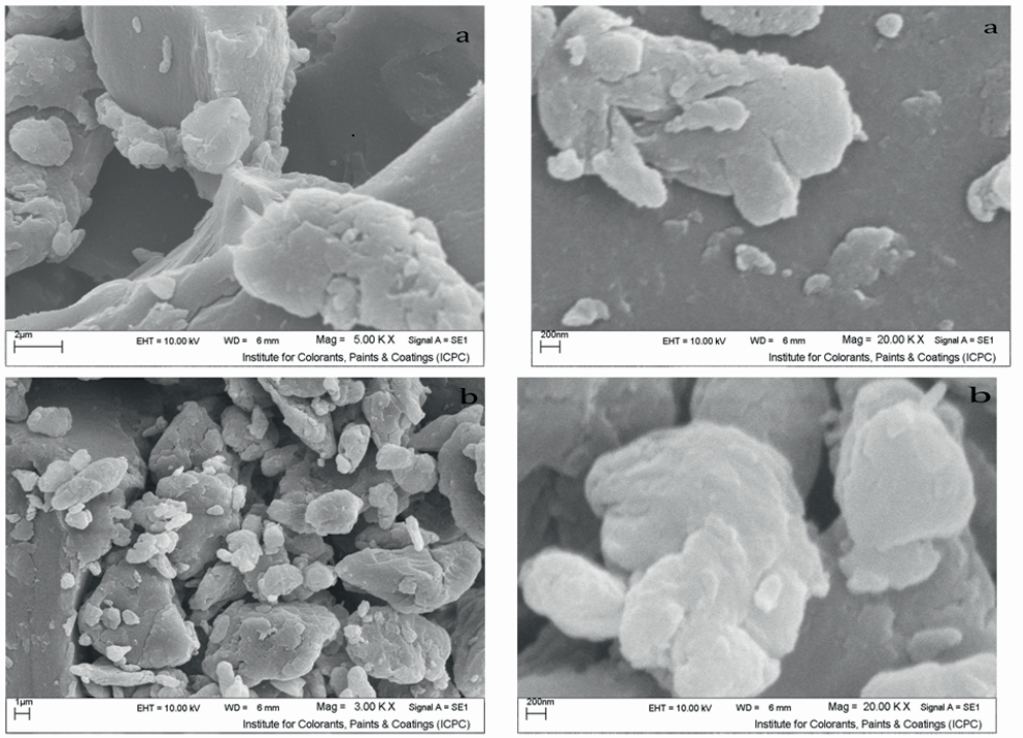

Figure 6. Scanning electron micrographs of PAI-nanocomposite films **5a** (a) and **5b** (b).

The first type is an intercalated polymer clay nanocomposite, which consists of well ordered multi layers of polymer chain and silicate layers a few nanometers thick. The second type is an exfoliated polymer-clay nanocomposite, in which is there is a loss of ordered structures due to the extensive penetration of polymer chain into the layer silicate. Such part would not produce distinct peaks in the XRD pattern [25]. In our PAI nanocomposite films there are coherent XRD signal at 5.30° and 4.85° related to 5 and 10 mass% nanocomposite films respectively.

3.4.3 Scanning Electron Microscopy

The surface morphology of the PAI-nanocomposite films prepared by solution intercalation technique is compared by SEM analyses. Figure 6 shows the morphological images of 5 and 10 mass% nanocomposite films respectively. The SEM images show that PAI matrix has a smooth morphology, where as the PAI matrix has amorph morphology. Also SEM micrographs of PAI-nanocomposite containing 5 and 10 mass% clay platelets were uniformly distributed without agglomeration.

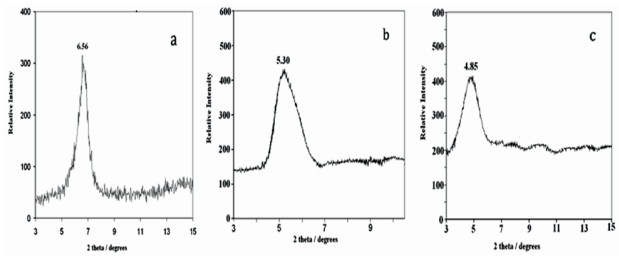

Figure 5. X-ray diffraction patterns of Organoclay (**a**), PAI-nanocomposite films **5a** (b) and **5b** (c).

3.4.4 Optical clarity of PAI-nanocomposite Films

Optical clarity of PAI-nanocomposite films containing 5 and 10 mass% clay platelets and neat PAI was compared by Uv-vis spectroscopy in the region of 300–800 nm. Figure 7 show the UV-vis transmission spectra of pure PAI and PAI-nanocomposite films containing 5 and 10 mass% clay platelets. These spectra show that the UV-visible region (250–800 nm) is affected by the presence of the clay particles and exhibiting low transparency reflected to the primarily intercalated composites. Results shows that the optical clarity of PAI-nanocomposite films system is significantly lower the neat PAI system.

3.4.5 Thermogravimetric Analysis

The thermal properties of PAI-nanocomposite films containing 5 and 10 mass% clay platelets and neat PAI were investigated by using TGA and DTG in nitrogen atmosphere at a rate of heating of 10 K/min, and thermal data are sum-

Polyimide	T_5 (K)[a]	T_{10} (K)[b]	Char Yield[c]	Water uptake (%)
5	144	176	46.2	9.3
5a	153	193	47.4	6.2
5b	303	370	57.4	3.4

[a,b] Temperature at which 5% and 10% weight loss was recorded by TGA at heating rate of 10 K/min in N_2 respectively.

[c] Percentage weight of material left undecomposed after TGA analysis 1073 K.

Table 2. Thermal behaviors and Water uptake of neat PAI **5** and PAI-nanocomposite films **5a** & **5b**.

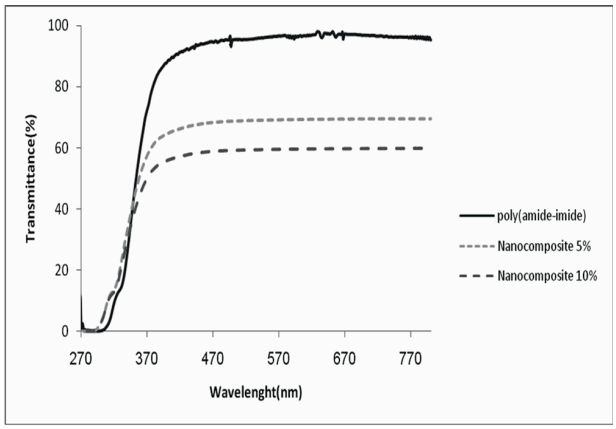

Figure 7. Uv-vis spectra of PAI **5**, PAI-nanocomposite films **5a** and **5b**.

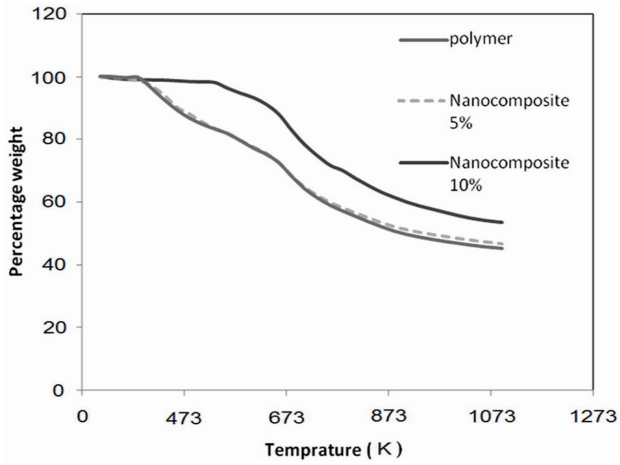

Figure 8. TGA thermograms of neat PAI **5** and PAI-nanocomposite films **5a** and **5b**.

marized in Table 2. These samples exhibited good resistance to thermal decomposition, up to 417–576 K in nitrogen, and began to decompose gradually above this temperature. T_5 for these polymers ranged from 417–576 K and T_{10} for them ranged from 449–643 K, and residual weights at 1073 K ranged from 46.2 and 57.4 % in nitrogen respectively. Incorporation of organoclay into the PAI matrix also enhanced the thermal stability of the nanocomposites. Figure 8 shows the TGA thermograms of PAI-nanocomposites under nitrogen atmosphere. Thus, we can speculate that interacting PAIs chains between the clay layers serve to improve the thermal stability of nanocomposites. The addition of organoclay in polymeric matrix can significantly improve the thermal stability of PAI.

3.4.6 Water Absorption Measurements

The PAI under investigation contains polar and cyclic imide rings and also polar amide groups in the backbone that have the tendency to uptake water through hydrogen bonding. Thus water absorption measurements become necessary for neat PAI **5** and PAI-nanocomposite films **5a** and **5b** and data are shown in Table 2. In the water permeability studies, we found that the incorporation of clay platelets into PAI matrix results in a decrease of water uptake relative to pure PAI by forming the tortuous path of water permeant. Water permeability depends on length, orientation and degree of delamination of layered silicate [28]. It should be noted that a further increase in clay concentration resulted in an enhanced barrier property of nanocomposites which may be attributed to the plate-like clays that effectively increase the length of the diffusion pathways, as well as decrease the water permeability.

4 Conclusions

The PAI-nanocomposites were successfully prepared using solution intercalation method. The structure and the uniform dispersion of organoclay throughout the PAI matrix were confirmed by FTIR, XRD and SEM analyses. The optical clarity and water absorption property of PAI-nanocomposites were decreased significantly with increasing the organoclay contents in PAI matrix. On the contrary the thermal stability of PAI-nanocomposites were increased significantly with increasing the organoclay contents in PAI matrix. The enhancements in the thermal stability of the nanocomposites films **5a** and **5b** caused by in-

troducing organoclay may be due to the strong interactions between polymeric matrix and organoclay generating well intercalation and dispersion of clay platelets in the PAI matrix.

References

[1] A. Usuki, M. Kawasumi, Y. Kojima, A. Okada, T. Kurauchi and O. Kamigaito, *J. Mater. Res*., **8** (1993), 1174–1178.

[2] A. Usuki, Y. Kojima, M. Kawasumi, A. Okada, Y. Fukushima, T. Kurauchi and O. Kamigaito, *J. Mater Res.*, **8** (1993), 1179–1184.

[3] Y. Kojima, A. Usuki, M. Kawasumi, A. Okada, Y. Fukushima, T. Kurauchi and O. Kamigaito, *J Mater Res.*, **8** (1993), 1185–1189.

[4] T. Lan, P. D. Kaviratna and T. Pinnavaia, *J Chem. Mater.*, **6** (1994), 573–575.

[5] P. B. Massersmith and E. P. Giannelis, *Chem Mater.*, **6** (1994), 1719–1725.

[6] H. L. Tyan, Y. C. Liu and K. H. T. Wei, *Chem. Mater.*, **11** (1999), 1942–1947.

[7] S. D. Burnside and E. P.Giannelis, *Chem. Mater.*, **7** (1995), 1597–1600.

[8] J. W. Gilman, C. L. Jackson, A. B. Morgan, R. J. Hayyis, E. Manias, E. P. Giannelis, M. Wuthenow, D. Hilton and S. H. Philips, *Chem. Mater.*, **12** (2000), 1866–1873.

[9] R. A. Vaia, S. Vasudevan, W. Krawiec, L. G. Scanlon and E. P. Giannelis, *Adv Mater.*, **7** (1995), 154–156.

[10] J. M. Yeh, S. J. Liou, C. Y. Lin, P. C. Wu and T. Y. Tsai, *Chem Mater.*, **13** (2001), 1131–1136.

[11] Y. H. Yu, J. M. Yeh, S. J. Liou and Y. P. Chang, *Acta Mater.*, **52** (2004), 475–486.

[12] K. Yano, A. Usuki, T. Kurauchi and O. Kamigaito, *J. Polym. Sci. Part A: Polym. Chem.* **31** (1993), 2493–2498.

[13] P. B. Messersmith and E. P. Giannelis, *J Polym Sci Part A: Polym Chem.*, **33** (1995), 1047–1057.

[14] L. Y. Jiang, C. M.Leu and K. H. Wei, *Adv Mater.*, **14** (2002), 426–429.

[15] Y. H. Zhang, Z. M. Dang, S. Y. Fu, J. H. Xin, J. G. Deng, J. Wu, S. Yang, L. F. Li and Q. Yan, *Chem Phys Lett.*, **401** (2005), 553–557.

[16] H. W. Wang, R. X. Dong, H. C. Chu, K. C. Chang and W. C. Lee, *Mater Chem Phys.*, **94** (2005), 42–51.

[17] W. A. Feld, B. Ramalingam and F. W. Harris, *J Polym Sci., Polym. Chem. Ed.*, **21** (1983), 319–328.

[18] Y. Imai, N. N. Maldar and M. Kakimoto, *J. Polym. Sci., Part A: Polym. Chem.*, **22** (1984), 2189–2196.

[19] R. Giesa, U. Keller and H. W. Schmidt, *ACS Polym Prepr.*, **33** (1992), 396–403.

[20] T. Y. Jadhav, J. Preston and W. R. Krigbaum, *J. Polym Sci, Part A: Polym Chem.*, **27** (1989), 1175–1179.

[21] K. Faghihi, M. Hajibeygi and M. Shabanian, *Macromol. Res.*, **18** (2010), 421–428.

[22] K. Faghihi, M. Shabanian and N. Emamdadi, *Macromol. Res.,* **18** (2010), 753–758.

[23] K. Faghihi, M. Shabanian and M. Hajibeygi, *Macromol. Res.*, **17** (2009), 912–918.

[24] Kh Faghihi, F. Shabani and M. Shabanian, *J. Macromol. Sci. Part A Pure Appl. Chem.*, **48** (2011), 381386.

[25] X. Fan, C. Xia and R. C. Advincula, *Colliod Surf A: Physicochem Eng Aspects*, **219** (2003), 75–86.

[26] C. M. Koo, S. O. Kim and I. J. Chung, *Macromolcules*., **36** (2003), 2758–2768.

[27] S. Mallakpour, A. R. Hajipour and S. Habibi, *J. Appl. Polym. Sci.*, **86** (2002), 2211–2216.

[28] S. Zulfiqar and M. I. Sarwar, *J. Incl. Phenom. Macrocycl. Chem*. **62** (2008), 353–361.